

2019-09

Microstructural ordering of nanofibers in flow-directed assembly

EnLai Gao, ShiJun Wang, ChuanHua Duan, ZhiPing Xu. 2019. "Microstructural ordering of nanofibers in flow-directed assembly." *Science China Technological Sciences*, Volume 62, Issue 9, pp. 1545 - 1554. <https://doi.org/10.1007/s11431-018-9421-5>

<https://hdl.handle.net/2144/41146>

"Downloaded from OpenBU. Boston University's institutional repository."

Supplementary Material for

Microstructural Ordering of Nanofibers in Flow-Directed Assembly

Enlai Gao^{1,4}, Shijun Wang^{1,4}, Chuanhua Duan^{2,*} and Zhiping Xu^{1,3,*}

¹Applied Mechanics Laboratory, Department of Engineering Mechanics, and Center for Nano and Micro Mechanics, Tsinghua University, Beijing 100084, China

²Department of Mechanical Engineering, Boston University, Boston, MA 02215, USA

³Applied Mechanics and Structure Safety Key Laboratory of Sichuan Province, School of Mechanics and Engineering, Southwest Jiaotong University, Chengdu 611756, China

⁴These authors contribute equally to this work.

*Corresponding authors. Emails: xuzp@tsinghua.edu.cn, duan@bu.edu

This **Supplementary Material** contains

- Model Parameterization in Dissipative Particle Dynamics (DPD) Simulations
- Integration Schemes for Solvent and Nanofiber Beads
- Simulating Shear Flow in DPD
- Simulating Solvent Evaporation in DPD
- Design the Fluidic Channel for Nanofiber Assembly

and

- A movie of simulated fiber assembly driven by flow and evaporation.

[M1.assembly.avi](#)

1. Model Parameterization in DPD Simulations

In general, a solvent bead corresponds to N_w water molecules, which defines the level of spatial coarse graining. Hence, a cube of volume R_c^3 contains $N_w\rho$ water molecules, where ρ is the number of DPD beads per cubic volume R_c^3 ($\rho = 3$ in this work). n is the number density of actual water molecules, in which $n = N_w\rho$. The mass of the DPD bead m equals $N_w m_w$, where m_w (18 g/mol) is the molecular mass of water. $k_B T$ equals 4.14×10^{-21} J, where k_B is the Boltzmann constant and T is the 300 K unless otherwise states in the rest.

1.1 Characteristic length scale R_c in DPD

As a water molecule occupies a volume of 30 \AA^3 , the volume of this coarsen cube is $30\rho N_m \text{ \AA}^3$, which corresponds to the density of water of 1000 kg/m^3 . Thus, the characteristic length scale R_c in the DPD model is defined as

$$R_c = (30\rho N_m)^{1/3} (\text{\AA}) \quad (\text{S1})$$

1.2 Characteristic time scale τ in DPD

Following the procedure to match the diffusion constant of pure water, outlined by Groot and Rabone [1], the characteristic time scale τ in DPD can be determined as

$$\tau = N_m D_b R_c^2 / D_w = 14.1 \pm 0.1 N_m^{5/3} (\text{ps}) \quad (\text{S2})$$

where D_b and D_w are the diffusion constant of DPD beads for water in the simulations and that of water molecules ($\sim 2.43 \pm 0.01 \times 10^{-5} \text{ cm}^2/\text{s}$) measured experimentally [2], respectively.

1.3 The value of parameter a

To find the value of the conservative force coefficient a in **Eq. 2**, we follow the procedure laid out by Groot *et al.* [1, 3], that is, we match the compressibility of the coarsen solvent with that of water (2.2 GPa). Through a series of equilibrium DPD simulations with different values of a and ρ , it is shown that the DPD equation of state derived, to a good approximation, can be given by

$$p = \rho k_B T + a a^2 \rho^2 \quad (\text{S3})$$

where the parameter α was determined to be 0.101 ± 0.001 . By definition, Keaveny *et al.* [4] gives the general case of the dimensionless isothermal compressibility κ^{-1} ,

$$\kappa^{-1} = (1 + 2\alpha a \rho / k_B T) / N_m \quad (\text{S4})$$

For water at 300 K, this dimensionless compressibility κ^{-1} has the numerical value 15.98. The isothermal compressibility κ_T^{-1} has the relation with the dimensionless isothermal compressibility κ^{-1} as,

$$\kappa_T^{-1} = n \kappa^{-1} k_B T / R_c^3 = 2.2 \text{ GPa} \quad (\text{S5})$$

Therefore, the value of a can be derived through **Eqs. S4** and **S5**. To verify the compressibility of DPD solvent, we conduct simulations at different coarse graining levels as shown in **Fig. S1a**, and the results fit well with the theoretical and experimental value (2.2 GPa).

To summarize, we derived the characteristic length scale R_c , mass scale m , time scale τ and the coefficient a in DPD at different coarse graining levels, by reproducing the density (1000 kg/m^3), diffusion coefficient ($2.43 \pm 0.01 \times 10^{-5} \text{ cm}^2/\text{s}$) and compressibility of water (2.2 GPa), which are listed in **Table S1**.

2. Integration Schemes for Solvent and Nanofiber Beads

For the velocity Verlet algorithm we use to integrate the equations of motion for the beads, time step size $\Delta t = 0.05\tau$ is an acceptable upper limit [1]. In addition, the time step sizes for nanofibers beads is also limited the by its highest vibrational frequency, which may further reduce the time step size due to the high stiffness of nanofibers compared to the soft repulsion between DPD beads of solvent. Considering the balance between numerical stability and the computational consumption, we use different time step sizes for DPD beads of solvent ($\sim 10^5$ beads) and nanofibers ($\sim 10^3$ beads), which is realized by the rRESPA multi-timescale integrator with 2 hierarchical levels, 0.005τ and 0.0001τ , respectively [5].

3. Simulating Shear Flow in DPD

The Lees-Edwards boundary [6] conditions are applied to generate Couette flow in the channel. Specifically, we shear the simulation box with a constant engineering

strain rate. The tilt in the flow direction (x) continues until the shear strain of 0.5 is reached, then the box flips to the shear strain of negative 0.5 while keeping the real coordinates and velocities of particles. Repeating this procedure generates a continuous shear flow. When a particle crosses a periodic boundary along y -axis, the difference of velocities between the low and high boundary is added (or subtracted) to its velocity correspondingly. This process produces the profile of velocity that linearly varies from at $y = 0$ to $y = L_y$, as validated in **Fig. S1b**.

The steady-state shear flow in our model is not suitable for conventional thermostats such as Nosé–Hoover thermostat and Langevin thermostat where temperature is regulated by feedback algorithms based on the absolute velocity of each particle, while DPD thermostat relies on the relative velocity between each pair of particles within short cut-off distance R_c , and temperature is regulated effectively with small errors. Hence, all simulations in this work run under the constant-temperature condition at 300 K using the DPD thermostat, which conserves the total momentum of system and correctly captures the hydrodynamical effects [1, 3].

4. Simulating Solvent Evaporation in DPD

To simulate the process of solvent evaporation, the solvent beads are removed in a controlled manner. Specifically, M solvent beads are chosen randomly in the simulation box and deleted every N steps. The evaporation rate can be controlled by the values of M and N . In addition, the density of the system keeps constant by adjusting the box volume to a new one considering the reduced mass of solvent through evaporation.

5. Design the Fluidic Channel for Nanofiber Assembly

5.1 Without solvent evaporation

The profile of 2D reducing fluidic channel can be described with two profiles as $h(x)$ and $-h(x)$, as shown in **Fig. 6a**. The width, pressure and flow rate at the inlet (outlet) are h_1 ($h_2 = \beta h_1$, where $\beta = h_2/h_1$ defines the width reduction of channel), p_1 (p_2) and

q_1 (q_2), respectively, and the length of the channel is L . From the Navier-Stokes equation for one dimensional and incompressible flow that disregards gravity and inertia forces, we have

$$\frac{d^2 u(x,y)}{dy^2} = \frac{1}{\mu} \frac{dp(x)}{dx} \quad (\text{S6})$$

where u , p and Δp ($\Delta p = p_1 - p_2$) are the flow velocity, pressure and pressure difference, respectively.

$$u(x,y) = \frac{1}{2\mu} \frac{dp(x)}{dx} y^2 + C_1 y + C_2 \quad (\text{S7})$$

Combined with the boundary conditions $u(x, y = \pm h(x)) = 0$, one can derive that

$$C_1 = 0$$

$$C_2 = \frac{1}{2\mu} \frac{dp(x)}{dx} h^2(x)$$

Hence, the distribution of the velocity in the channel is

$$u(x,y) = \frac{1}{2\mu} \frac{dp(x)}{dx} [y^2 - h^2(x)] \quad (\text{S8})$$

The flow rate can be expressed from **Eq. S8** based on the equation of continuity, $q(x) = q_1 = q_2$ with the absence of evaporation,

$$q(x) = d \int_{-h(x)}^{h(x)} u(x,y) dy = d \int_{-h(x)}^{h(x)} \frac{1}{2\mu} \frac{dp(x)}{dx} [y^2 - h^2(x)] dy = -\frac{2d}{3\mu} \frac{dp(x)}{dx} h^3(x) \quad (\text{S9})$$

Here d is the depth of the flow channel. For simplicity, take $h(x)$ as $h_1 - x \tan \alpha$, then $dh = -d x \tan \alpha$, and then

$$\frac{dp(x)}{dh(x)} = \frac{3\mu q_1}{2d h^3(x) \tan \alpha} \quad (\text{S10})$$

By solving the integrals in **Eq. S10**, we have,

$$p(x) = -\frac{3\mu q_1}{4d h^2(x) \tan \alpha} + C$$

Combined with the boundary conditions, $h = h_1, p = p_1; h = h_2, p = p_2; p_1 - p_2 = \Delta p$, one can derive that

$$C = p_1 + \frac{3\mu q_1}{4dh_1^2 \tan \alpha}$$

The distribution of the pressure, flow rate, velocity and velocity gradient of flow along the channel can then be expressed,

$$p(x) = p_1 - \frac{[h_1/h(x)]^2 - 1}{(h_1/h_2)^2 - 1} \Delta p \quad (\text{S11})$$

$$q(x) = \frac{4dh_1^2 h_2^2}{3\mu L (h_1 + h_2)} \Delta p = q_1 = q_2 \quad (\text{S12})$$

$$u(x, y) = \frac{\Delta p}{\mu L} \frac{h_1^2 h_2^2}{(h_1 + h_2) h^3(x)} [h^2(x) - y^2] \quad (\text{S13})$$

$$\frac{du(x, y)}{dy} = -\frac{2\Delta p}{\mu L} \frac{h_1^2 h_2^2}{(h_1 + h_2) h^3(x)} y \quad (\text{S14})$$

The distribution of average shear rate along the channel significantly affects the orientational order of nanofibers in the flow, that is

$$\dot{\gamma}(x) = \frac{q(x)}{dh^2(x)} = \frac{4h_1^2 h_2^2}{3\mu (h_1 + h_2)} \frac{\Delta p}{L} \frac{1}{h^2(x)} \quad (\text{S15})$$

When the cross section of channel is uniform, or $h_1 = h_2 = h$,

$$\dot{\gamma} = \frac{2h \Delta p}{3\mu L} \quad (\text{S16})$$

5.2 With solvent evaporation

With solvent evaporation, a supplementary condition is introduced that satisfies the mass conservation of flow. With the assumption that the total evaporation rate $q_e = \lambda A$ is proportional to the flow area swept from the inlet to x along the channel, $A = [h_1^2 - h(x)^2]/\tan \alpha$, the linear evaporation intensity coefficient λ defines the intensity of evaporation. Hence, the flow rate $q(x)$ at position x can then be expressed as

$$q(x) = q_1 - q_e(x) = q_1 - \lambda \frac{h_1^2 - h^2(x)}{\tan \alpha} \quad (\text{S17})$$

The distribution of average shear rate along the channel is then modified from **Eq. S15** as

$$\dot{\gamma}(x) = \frac{q(x)}{dh^2(x)} = \left[q_1 - \lambda \frac{h_1^2 - h^2(x)}{\tan \alpha} \right] / [dh^2(x)] \quad (\text{S18})$$

In the strong-evaporation limit where the solvent at outlet vanishes,

$$q_2 = q_1 - q_e(L) = q_1 - \lambda \frac{h_1^2 - h_2^2}{\tan \alpha} \approx 0 \quad (\text{S19})$$

Then we have

$$q_1 = \lambda \frac{h_1^2 - h_2^2}{\tan \alpha}$$
$$q(x) = q_1 - q_e(x) = \lambda \frac{h^2(x) - h_2^2}{\tan \alpha} \quad (\text{S20})$$

and

$$\dot{\gamma}(x) = \frac{q(x)}{wh^2(x)} = \frac{q_1}{w(h_1^2 - h_2^2)} [1 - h_2^2/h^2(x)] \quad (\text{S21})$$

Eqs. S15 and **S21** are thus the two extreme cases that correspond to conditions of evaporation-absent and strong evaporation limits, respectively, as derived from **Eq. S18**.

Tables, Figures and Captions

Table S1 Characteristic length scale R_c , mass scale m , time scale τ and a at different coarse graining levels in DPD.

N_m	R_c (Å)	m (g/mol)	τ (ps)	a
1	4.48	18	14	16
3	6.46	54	88	78
9	9.32	162	549	238

Table S2 Model parameters for beads in the nanofiber.

Parameters	Values
Equilibrium bead distance R_0 (Å)	14
Tensile stiffness parameter K_T (kcal mol ⁻¹ Å ⁻²)	19656
Bending stiffness parameter K_B (kcal/mol)	29250357
12-6 Lennard-Jones parameter ϵ (kcal/mol)	218
12-6 Lennard-Jones parameter σ (Å)	21

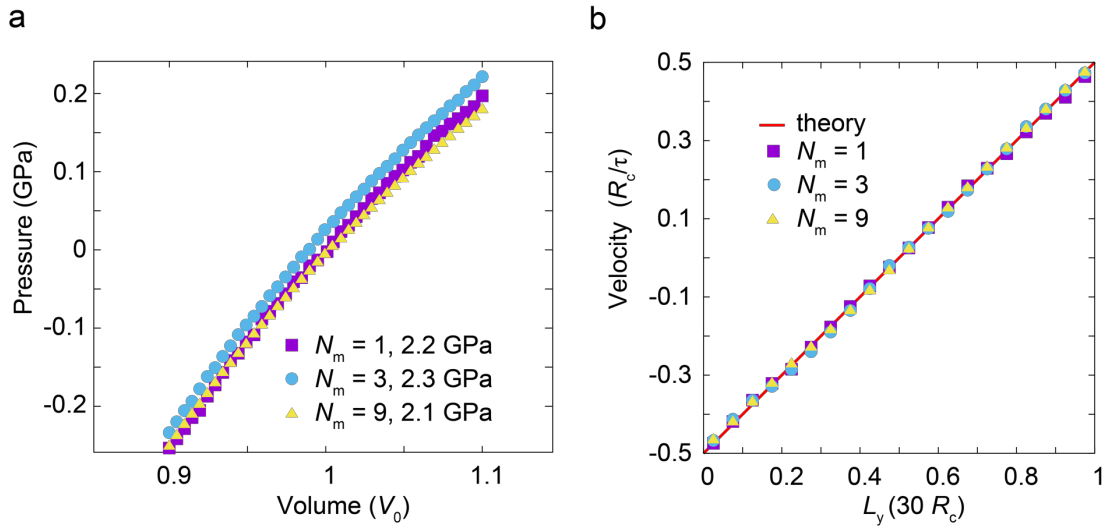


Figure S1 (a) Pressure-volume relation of the DPD solvent, to verify the bulk modulus of water (2.2 GPa) at different coarse-grain levels ($N_m = 1, 3, 9$). (b) A typical velocity profile along y direction (perpendicular to the flow direction) in the shear flow DPD simulations. The profile is obtained by averaging the velocity of DPD beads within 20 different bins with height $1.5R_c$ in the y direction, after the steady state has been reached. DPD simulations for this data are conducted with a box of $30R_c \times 30R_c \times 30R_c$ and a shear rate of $0.33\tau^{-1}$.

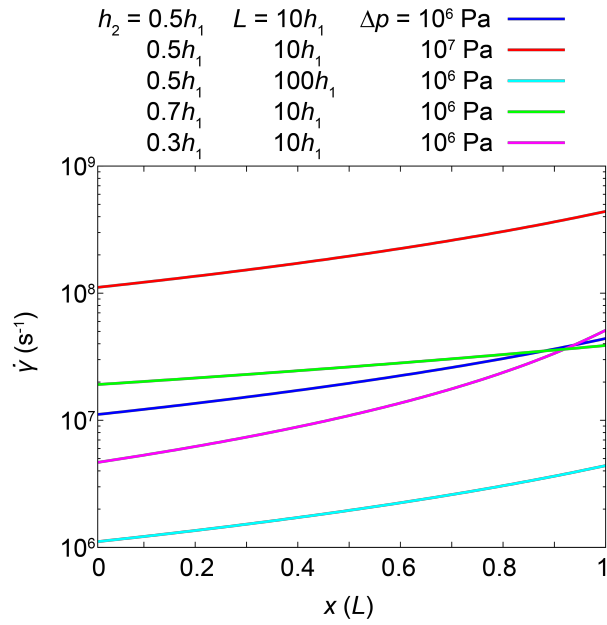


Figure S2 The distribution of average shear rate $\dot{\gamma}(x)$ along the channel, plotted as functions of the pressure difference Δp across the channel, that is $p_1 - p_2$, the length L and width h of the channel (**Eq. S15**). The pressure gradient indicates the energy consumption in the process.

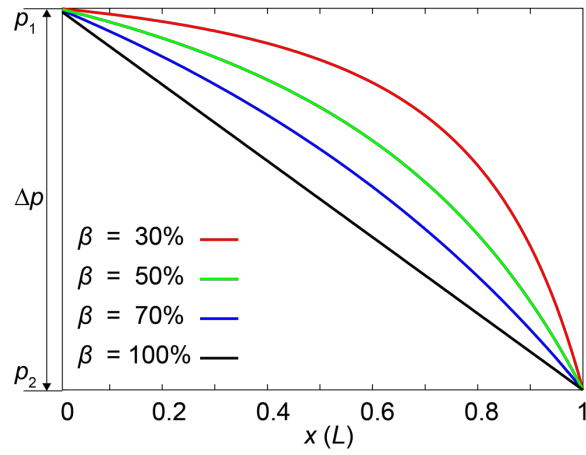


Figure S3 The distribution of pressure along flow channel, plotted for different values of $\beta = h_2/h_1$. The pressure gradient indicates the energy consumption in the process.

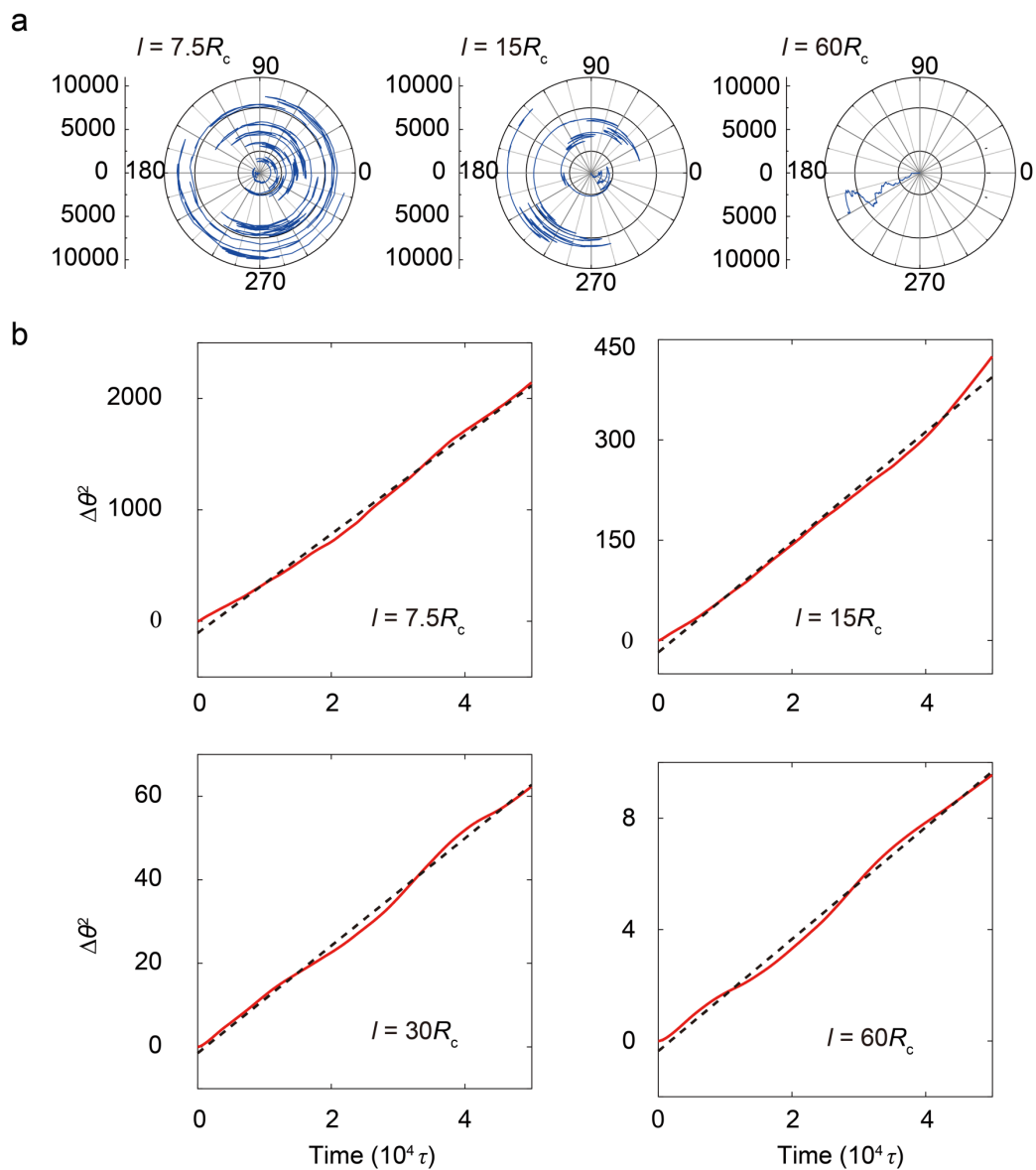


Figure S4 (a) The rotational Brownian motion of nanofibers in the polar coordinates. (b) The angular mean square displacement of nanofibers plotted as a function of time, where the slope gives rotational diffusion coefficients. The effect of nanofiber length is clearly demonstrated through these data from DPD simulations.

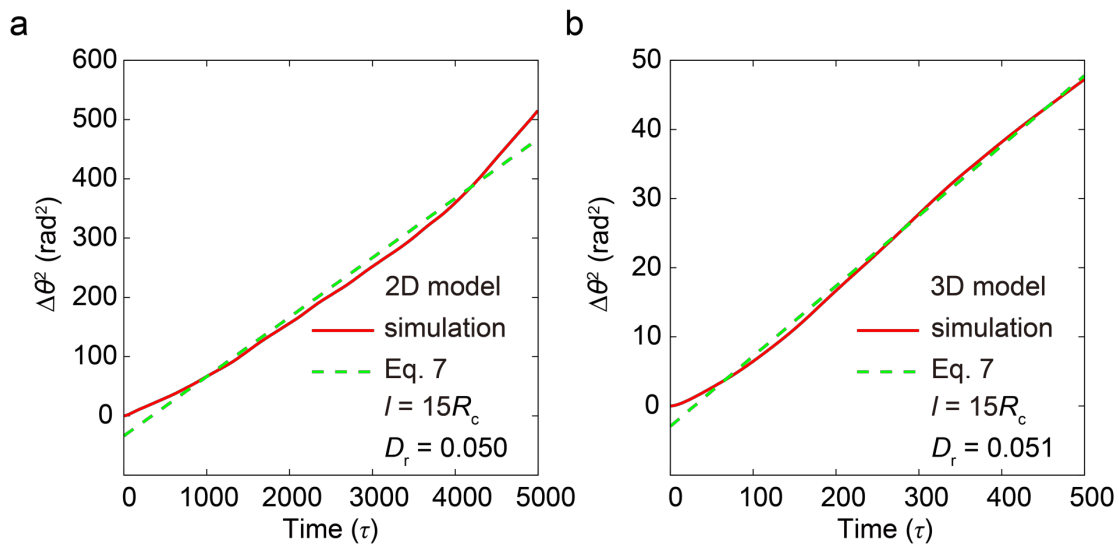


Figure S5. Mean square deviation of the nanofiber orientation obtained from 2D (a) and 3D (b) DPD simulations. The orientation of nanofibers in 3D models is projected to the 2D plane for comparison with panel (a).

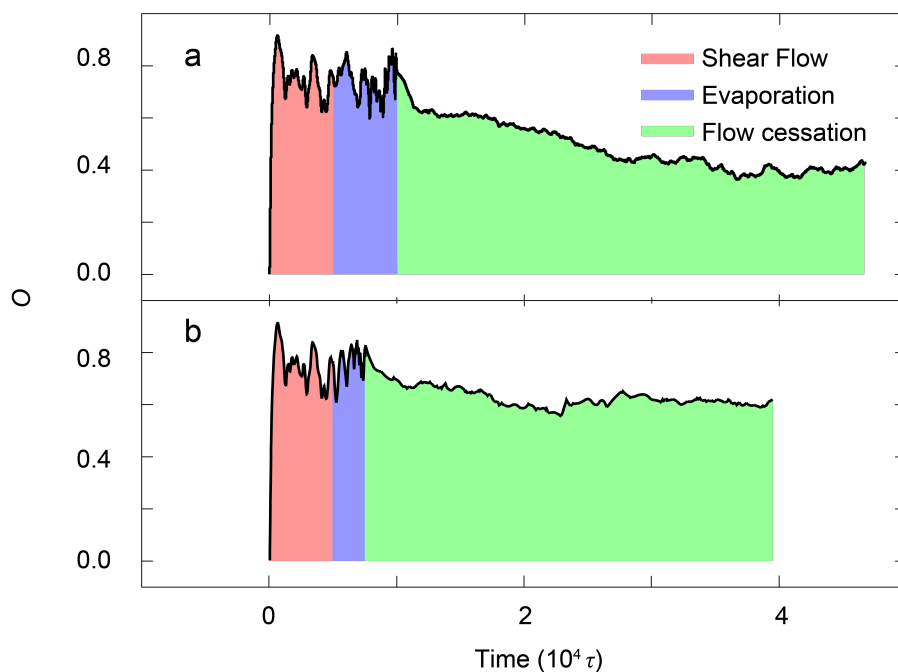


Figure S6. Orientational order evolution in nanofiber assemblies at different evaporation rates. After a shear flow ($t = 0 \sim 0.5 \times 10^3 \tau$), 85 % of the solvents are evaporated within (a) $0.5 \times 10^3 \tau$ and (b) $0.25 \times 10^3 \tau$. The results show that, after the shear flow cessation, the value of O approaches a constant of (a) ~ 0.4 and (b) ~ 0.6 , respectively. The light-red, blue and green regions indicate the three distinct stages of steady shear flow, solvent evaporation and flow cessation.

References

- 1 Groot R D and Rabone K L. Mesoscopic simulation of cell membrane damage, morphology change and rupture by nonionic surfactants. *Biophys J*, 2001, 81: 725-736
- 2 Partington J R, Hudson R F and Bagnall K W. Self-diffusion of aliphatic alcohols. *Nature*, 1952, 169: 583-584
- 3 Groot R D and Warren P B. Dissipative particle dynamics: Bridging the gap between atomistic and mesoscopic simulation. *J Chem Phys*, 1997, 107: 4423-4435
- 4 Keaveny E E, Pivkin I V, Maxey M, et al. A comparative study between dissipative particle dynamics and molecular dynamics for simple- and complex-geometry flows. *J Chem Phys*, 2005, 123: 104107
- 5 Tuckerman M, Berne B J and Martyna G J. Reversible multiple time scale molecular-dynamics. *J Chem Phys*, 1992, 97: 1990-2001
- 6 Lees A W and Edwards S F. The computer study of transport processes under extreme conditions. *J Phys C: Solid State Phys*, 1972, 5: 1921-1928